



Scaling of energy dissipation in crushing and fragmentation: a fractal and statistical analysis based on particle size distribution

ALBERTO CARPINTERI, GIUSEPPE LACIDOGNA and NICOLA PUGNO

Department of Structural Engineering and Geotechnics, Politecnico di Torino, Corso Duca degli Abruzzi 24, 10129 Torino, Italy

Received 17 July 2003; accepted in revised form 16 March 2004

Abstract. An extensive experimental investigation on concrete specimens under crushing and fragmentation over a large scale range (1:10) – exploring even very small specimen dimensions (1 cm) – was carried out to evaluate the influence of fragment size distribution on energy density dissipation and related size effect. To obtain a statistically significant fragment production as well as the total energy dissipated in a given specimen, the experimental procedure was unusually carried out up to a strain of approximately –95%, practically corresponding to the initial fragment compaction between the loading platens. The experimental fragment analysis suggests a fractal law for the distribution in particle size; this simply means that fragments derived from a given specimen appear geometrically self-similar at each observation scale. In addition, clear size effects on dissipated energy density are experimentally observed. Fractal concepts permit to quantify the correlation between fragment size distribution and size effect on dissipated energy density, the latter being governed by the total surface area of produced fragments. The experimental results agree with the proposed multi-scale interpretation satisfactorily.

Key words: Energy dissipation, fragmentation, scaling particle size, size effects.

1. Introduction

The dependence of dissipated energy density in compression on specimen size, as obtained from the experimental investigation described by Carpinteri and Ferro (2002), is essential in energy-based failure criteria. Even if an extensive literature treats this specific topic, a rigorous physical interpretation quantifying the size effect on energy density is missing. Ductility (or energy density dissipation) increases by decreasing the specimen size. The same trend can be observed also with respect to the specimen slenderness. In addition, it is important to highlight the friction (between specimen and loading platens) influence. Usually, the presence of friction induces a considerable increase in strength by decreasing the size or slenderness; the same trend appears to be very mitigated or even absent in frictionless tests. On the other hand, friction does not seem to play an important role on energy density. Experimental, numerical as well as theoretical investigations on size and shape effects are reported in the papers by Carpinteri, Ciola, Pugno, Ferrara, Gobbi (2001), Carpinteri, Ciola, Pugno (2001), Carpinteri and Pugno (2001, 2002a).

In general, the constitutive relations and the mechanical parameters for concrete are obtained from standard specimens. The introduction of high-strength concrete, with a compression strength up to five times the standard strength, should suggest the use of smaller specimens, with the advantages of maintaining the use of standard test machines available in the laboratories, of easy handling and of using less concrete. Another important opportunity for reducing specimen sizes is constituted by the determination of the concrete strength for

existing structures by drilling small specimens. This technique is very useful, the deterioration of the mechanical properties of concrete structures being one of the main problems in Civil Engineering.

The choice of the standard size and shape is affected by the variations of the compressive strength with size-scale and with height/diameter (or slenderness) ratio. These variations are consistent when the rigid test machine platens are in direct contact with the concrete specimen, the lateral deformation of concrete being restrained at the specimen ends (Carpinteri et al., 1999). In that case, the conclusion is that, in order to evaluate the compressive strength of concrete objectively, a specimen size larger than the maximum aggregate size by one order of magnitude has to be considered. The effect of size on the mechanical properties of concrete is also important when small scale models are used to predict the behavior of real structures. Early work on the size effect in compression dates back to the 1920's. Gonnemann (1925) emphasized the size effects through an extensive investigation on the compressive strength of cylinders with a height/diameter ratio equal to two. Many other authors fronted the problem of size effects on nominal strength for concrete in compression. Blanks and McNamara (1935) performed tests on cylindrical specimens with slenderness of 2 in a large scale range (1:12), while Jishan and Xixi (1990) performed experiments on cubes (scale range 1:4) and on prisms with a slenderness of 3 (scale range 1:3).

Usually, the nominal compressive strength is obtained by dividing the peak force by the specimen cross-section area. This operation has the meaning of estimating a global material property, ignoring at the same time the material structure as well as the material failure behavior during the test. Kotsovos (1989) performed experiments on cylinders with an aspect ratio of 2.5 and with different frictional systems. He observed the same pre-peak behavior (in dimensionless form) for the different choices of loading system, and post-peak dimensionless stress-displacement curves characterized by increasing slope with decreasing the coefficient of friction. The friction system adopted in the compression tests (Carpinteri and Ferro, 2002) comes out from the analysis of the RILEM Technical Committee (TC) 148 SSC results (RILEM, 1997). The purpose of this TC, which involved 11 laboratories, was that of defining a standardised test method for describing compressive softening in concrete. The loading platens, they found, not only affect the post-peak behavior, but also the peak stress. The suggestion from Delft Technical University (van Vliet and van Mier, 1996) was to use a newly developed teflon layer (comprising two 100 μm thick sheets of teflon foil, with 50 μm of hearing grease in between) or rigid steel platens as loading systems to test prismatic normal strength or high-strength concrete specimens with different slenderness (equals to 0.5, 1.0, 2.0). They observed an increase in peak stress by decreasing the slenderness (up to 200%), when the specimens were loaded between rigid steel platens, whereas an almost constant peak stress was found with the application of teflon interlayers. The softening branch, with both the systems, becomes steeper with increasing specimen height. These results suggested to Carpinteri and Ferro (2002) to use two teflon layers of 150 μm thickness with oil in between and a specimen slenderness equal to one.

Momber (2000) analyzed the fragmentation of standard concrete cylinders under compression. He observed how the standard codes (ASTM C39-86) consider types of failure which involve only large *primary* fracture debris. He noticed also how, after compression testing of any concrete specimen, fragments of fine-grained material are generated, which are usually called *secondary* fracture debris. He emphasized the role of the second fracture debris under compression. Fragments usually appear geometrically self-similar at each observation scale (Turcotte, 1992). A powerful mathematical tool to study self-similar objects is the Fractal

Geometry. It was applied by Carpinteri (1994) to derive a scaling law on nominal strength that is frequently applied by different authors in the interpretation of test data (Burtscher and Kollegger, 2003). On the other hand, Fractal Geometry is herein applied to give an interesting multi-scale interpretation of the mentioned energy size effect. We will refer to the fractal fragmentation theory, only recently developed (Carpinteri and Pugno 2002a,b, 2003).

2. Fractal and statistical analysis

After crushing, the probability density function $p(r)$, which, multiplied by the interval amplitude dr represents the percentage of fragments with size between r and $r + dr$, can be assumed to present a fractal form (Carpinteri and Pugno, 2002a,b):

$$p(r) = D \frac{r_{\min}^D}{r^{D+1}}, \quad (1)$$

where $r_{\min} \ll r_{\max}$ and D is the so called fractal exponent, usually comprised between 2 and 3.

Let us assume a smallest fragment of size $r_{\min} = \text{constant} \neq 0$ and the hypothesis of self-similarity for the largest one, i.e., $r_{\max} \propto L$, L being a characteristic size of the specimen under crushing. The energy density ψ will be basically dissipated into (i) friction between the fragment surfaces and (ii) to produce the new free surface. It is expected to be proportional to the total surface area of fragments (over the fragmented volume) as discussed by Carpinteri and Pugno (2002a, b) and can be obtained by integration of the total surface and volume of fragments, starting from Equation (1), as demonstrated by Carpinteri and Pugno (2002a, b):

$$\psi \propto L^{D-3} \quad (2)$$

It represents the correlation between particle size distribution and energy size effect. Note that an identical equation was reported by Nagahama (1993) and Nagahama and Yoshii (1993), simply assuming an energy dissipation occurring in a fractal surface $\propto L^D$. As a matter of fact, in these interesting papers the law of Equation (2) was assumed, to fit the three well-known comminution laws corresponding to $D = 2, 2.5$ and 3 (see Carpinteri and Pugno 2002a, b), rather than demonstrated. Only for the particular case of $D = 3$ the energy density appears to be – as usually assumed – size-independent. Jaeger et al. (1986) reported that a considerable percentage of the energy usually assumed to be dissipated to form new surface is actually absorbed by internal damage. Even if we think that friction rather than internal damage is the predominant cause of energy dissipation in comminution, the fact that a constant percentage with respect to the dissipated energy in pure free surface production can be defined, agrees with the previous hypothesis of energy dissipation proportional to the surface of fragments.

Equation (1) can be integrated to compute the mass of particles with radius smaller than r , so that the ratio of this partial mass to the total mass of fragments becomes (Carpinteri and Pugno, 2003):

$$\frac{M(< r)}{M} \cong \left(\frac{r}{r_{\max}} \right)^{3-D} \quad (3)$$

Through an experimental statistical fragment analysis, we are able to quantify the exponent $D-3$ in Equation (3), representing the slope in the bilogarithmic diagram relative mass vs relative size of fragments. It should represent the negative slope (in a bilogarithmic diagram)

of the size effect on energy density dissipation, as suggested by Equation (2). The energy density can be experimentally deduced simply considering the area under the full stress σ versus strain ε curve (elastic and softening branches) obtained during the compression test. The experimental correlation between particle size distribution and size effect on dissipated energy density is theoretically described introducing the fractal exponent D obtained from Equation (3) into Equation (2). It gives:

$$\int \sigma d\varepsilon = \psi \propto L^{-\log \frac{M(<r)}{M} / \log \frac{r}{r_{\max}}} = L^{D-3} \quad (4)$$

Validation of Equation (4) is the purpose of the present paper. Equation (4) is the result of the previous fractal and statistical analysis. The physical meaning is the following: the fragments, which are self-similar at each scale, imply an energy dissipation over a fractal set with fractal dimension D comprised between 2 and 3. Consequently, the dissipated energy density will be strongly affected by scale effects; it only vanishes in the particular case of energy dissipation in a volume ($D = 3$).

3. Experimental assessment

The ambition of testing concrete specimens in compression over a very wide size range is hardly consistent with the set-up, which opposes physical limits. The fundamental idea was to use a simple standard testing apparatus. This apparatus has been also improved by the authors, introducing acoustic emission instruments, to take into account the evolution of the energy dissipation and not only its final value (Carpinteri, Lacidogna, Pugno, 2003). The experimental apparatus is composed by a closed-loop servo-hydraulic system and by strain gauges glued on the specimen to record longitudinal and transversal deformation. The energy density dissipated in crushing is given by $\psi = \int \sigma d\varepsilon$.

The experimental analysis on energy density dissipation was carried out by Carpinteri and Ferro (2002); for details on concrete properties and stress-strain curves, the reader should refer to this paper. The specimens were cylinders with a height/diameter ratio equal to 1 and a diameter, chosen as the characteristic size, equal to 1, 2.3, 4.5 and 10 cm. The four considered different diameters were in a scale range of 1:10. Six specimens were tested for the diameter of 1 (C1), 2.3 (C2) and 4.5 (C3) cm and four specimens for the diameter of 10 cm (C4).

The first problem was that of defining the size and the slenderness of the test specimens. The size is limited by the dimension of the aggregates (lower limit) and by the potentialities of the available equipment (upper limit). The concrete used for the specimens is characterized by a maximum aggregate size of 4 mm. All the cylinder specimens were obtained by drilling from a unique concrete block. The water-cement ratio is equal to 0.65 as well as the porosity is of 17.7% in volume for a nominal strength of 52 N/mm².

For the three smallest sizes, cylinders with diameters 1 (C1), 2.3 (C2) and 4.5 cm (C3), the tests were carried out on a uniaxial compression machine with a capacity of 100 kN. We have to emphasize that the aggregate size of 4-mm represents the upperbound aggregate dimension. Practically, from a statistical viewpoint, we expect smaller maximum aggregate size in the smallest specimens, so that also their volumes were considered representative. The sizes of the loading platens and of the specimens were the same. This was done to eliminate the fragmentation of the fully developed fragments, considering this effect out of the real resistance of the specimen.

Table 1. Experimental energy density dissipation (N/mm^2).

C1	C2	C3	C4
6.12	2.51	1.33	0.42
7.32	3.45	2.90	–
7.12	2.75	2.62	–
8.34	2.78	3.24	–

The machine is controlled by a closed-loop servo-hydraulic system. Of the two loading platens, the lower is fixed whereas the upper is connected to the machine hinge. In this way, the upper platen can adjust to the geometrical imperfections of the specimen. All compression tests with this machine were performed under displacement control, by imposing a constant rate in the displacement of the upper loading platen. The displacement rate was set in order to impose the same stress rate to all the specimen sizes. A stress rate equal to $0.5 \text{ Nmm}^{-2} \text{ s}^{-1}$ was adopted, as prescribed by the UNI Standard 6130 for cubic strength evaluation. On each specimen two bidirectional strain gauges were glued, the lengths of which were taken proportional to the specimen height. The axial deformation, as well as the lateral deformation in the middle part of the specimen, were measured with the strain gauges.

The experimental results on energy density dissipation under crushing are summarized in Table 1. Unfortunately, only for one specimen C4 it was possible to capture the softening branch. The introduction of a teflon layer strongly reduced the size effect on nominal strength, which appears nearly size-independent.

The statistical particle size analyses were carried out by a standard vibrating machine with six in series different sieves. Three steps for each specimen were considered to investigate over 18 different fragment sizes through corresponding sieves with square mesh size of 60, 50, 40, 30, 25, 20, 15, 10, 8, 7, 6, 5, 4, 3, 2, 0.5, 0.2 and 0.1 mm. As an example, the fragments derived from crushing are shown in Figure 1. On the other hand, the fragment analyses of the four different specimen sizes are reported in the diagrams of Figures 2–5, i.e. the diagram of Equation (3).

The largest size will be neglected in the following considerations. The slope of the diagrams size vs. mass of fragments (specimens C1, C2 and C3) appears nearly constant with a mean value of 0.71. This value, as argued in Section 2, should be close to the theoretical slope in a bilogarithmic diagram energy density vs. size. The size effect on energy density, according to Table 1 and Equation (2), is described in Figure 6. Even if the experimental scattering is rather large, the trend is clear. The negative slope appears to be approximately equal to 0.75 and close to the value of 0.71 suggested by the fractal and statistical analysis of fragment size.

The experimental results seem to confirm the correlation between fragmentation and energy density dissipation described by Equation (4). Clearly, it is the softening branch, where the fragmentation is acute, that mainly contributes to the fractal character of the energy dissipation.



Figure 1. Fragments from the specimen of size 10 cm.

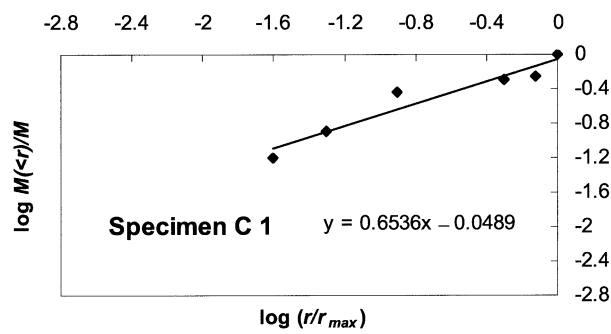


Figure 2. Relative size vs relative mass of fragments for the specimen of size 1 cm.

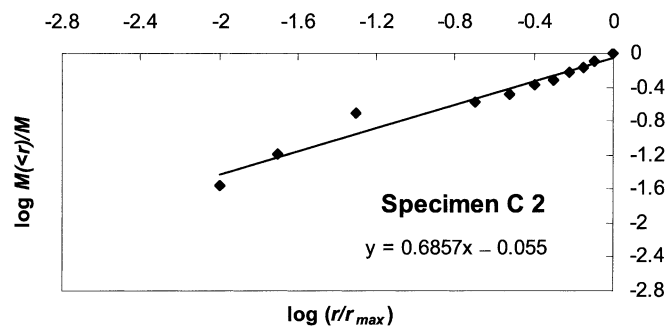


Figure 3. Relative size vs relative mass of fragments for the specimen of size 2.3 cm.

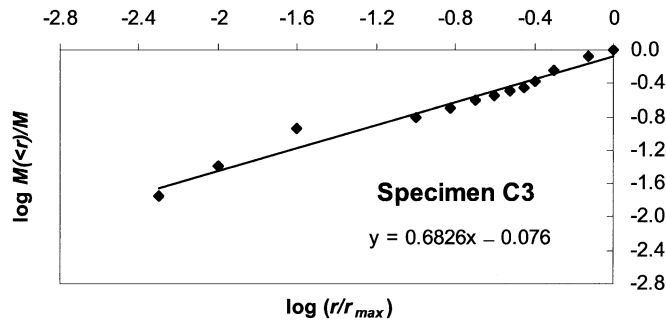


Figure 4. Relative size vs relative mass of fragments for the specimen of size 4.5 cm.

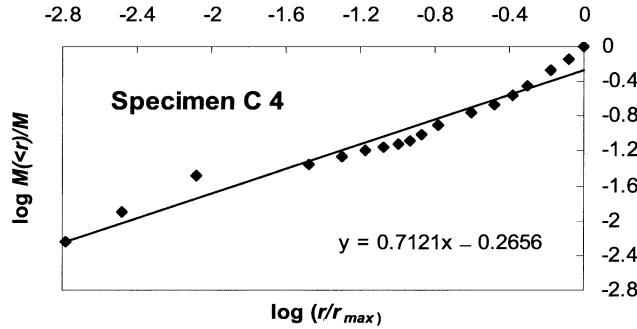


Figure 5. Relative size vs relative mass of fragments for the specimen of size 10 cm.

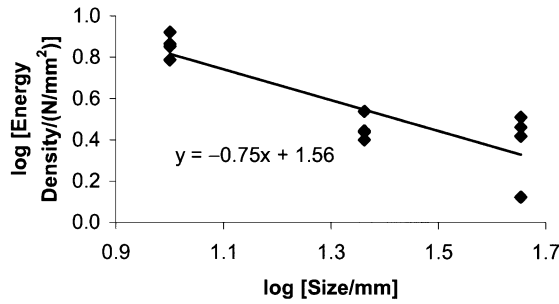


Figure 6. Size effect on dissipated energy density.

4. Conclusions

The fractal and statistical analysis has shown how the size effects on dissipated energy density are strictly connected to the fractal domain in which the dissipation occurs. It has been assumed to occur locally over the fragment surface as the case of friction and crack formation energy dissipations. The correlation is quantified by Equation (4). This seems to be confirmed by the experiments on energy density dissipation and particle size distribution analysis (even if the roles of frictional energy and internal fragment dissipations remain not well understood). The physical meaning is that fragments, being self-similar at each scale, imply an energy dissipation in a fractal set having fractal dimension D comprised between 2 and 3. Only for the limit case of dissipation in a volume ($D = 3$), the size effect should vanish. On the other hand, the experimental results show a fractal dimension closer to that of a surface rather than a volume. This result suggests a stress-displacement rather than a stress-strain universal relation,

according to the observations by van Mier (1986). However, the correct interpretation of this phenomenon goes through the fractal dimension of the topological set of dissipation rather than a trivial displacement localisation.

Acknowledgements

The present research was carried out with the financial support of Ministry of University and Scientific Research (MIUR) and the National Research Council (CNR).

References

- Blanks, R.F. and McNamara, C.C. (1938). Mass concrete tests in large cylinders. *Journal of American Concrete Institute* **31**, 280–303.
- Burtscher, S.L. and Kollegger, J. (2003). Size effect of sandstone and concrete. Computational Modelling of Concrete Structures, Bicanic et al. (eds).
- Campione, G. and Mindess, S. (1999). Size effects in compression of high strength fibre reinforced concrete cylinders subjected to concentric and eccentric loads, in *Materials for Buildings and Structures, Euromat 99*, (edited by F.H. Wittmann), DGM and WILEY-VCH, 6 86–91.
- Carpinteri, A. (1994). Scaling laws and renormalization groups for strength and toughness of disordered materials. *International Journal of Solids and Structures* **31**, 291–302.
- Carpinteri, A. and Ferro, G. (2002). Scale dependence of the dissipated energy density in compression, in International Conference on New Challenges in Mesomechanics, August 23–30, Aalborg University, Denmark.
- Carpinteri, A. and N. Pugno (2001). Friction and specimen slenderness influences on dissipated energy density of quasi-brittle materials in compression: an explanation based on fractal fragmentation theory, in International Conference on Fracture Mechanics of Concrete Structures – 4, May 28 – June 2, Cachan, France.
- Carpinteri, A. and Pugno, N. (2002a). Fractal fragmentation theory for shape effects of quasi-brittle materials in compression. *Magazine of Concrete Research* **54**(6), 473–480.
- Carpinteri, A. and Pugno, N. (2002b). One-, two- and three-dimensional universal laws for fragmentation due to impact and explosion. *Journal of Applied Mechanics* **69**, 854–856.
- Carpinteri, A. and Pugno, N. (2003). A Multifractal comminution approach for drilling scaling laws. *Powder Technology* **131**, 93–98.
- Carpinteri, A., Ciola, F. and Pugno, N. (2001). Boundary element method for the strain-softening response of quasi-brittle materials in compression. *Computers and Structures* **79**, 389–401.
- Carpinteri, A., Ferro, G. and Monetto, J. (1999). Scale effects in uniaxially compressed concrete specimens. *Magazine of Concrete Research* **51**, 217–225.
- Carpinteri, A., Lacidogna, G. and Pugno, N. (2003). Acoustic emissions to evaluate the energy dissipation during compression of heterogeneous materials, Proc. of the X Int. Con. on Sound and Vibration, July 7–10, Stockholm, Sweden.
- Carpinteri, A., Ciola, F., Pugno, N., Ferrara, G. and Gobbi, M.E. (2001). Size-scale and slenderness influence on the compressive strain-softening behaviour of concrete: Experimental and numerical analysis. *Fatigue and Fracture of Engineering Materials and Structures* **24**, 441–450.
- Gonnerman, H.F. (1925). Effect of size and shape of test specimen on compressive strength of concrete. *Proceedings ASTM* **25**, 237–250.
- Jaeger, Z., Englman, R., Gur, Y. and Sprecher, A. (1986). Internal damage in fragments. *Journal of Material Sciences Letters* **5**, 577–579.
- Jishan, X. and Xixi, H. (1990). Size effect on the strength of a concrete member. *Engineering Fracture Mechanics* **35**, 687–695.
- Kotsovos, M.D. (1989). Effect of testing techniques on the post-ultimate behavior of concrete in compression. *Materials and Structures (RILEM)* **16**, 3–12.
- Momber, A.W. (2000). The fragmentation of standard concrete cylinders under compression: the role of the secondary fracture debris. *Engineering Fracture Mechanics* **67**, 445–459.

- Nagahama, N. (1993). Fractal fragment size distribution for brittle rocks. *International Journal Rock Mechanics Min. Science and Geomechanical Abstracts* **30**, 469–471.
- Nagahama, N. and Yoshii, K. (1993). Fractal dimension and fracture brittle rocks. *International Journal of Rock Mechanics Min. Science and Geomechanical Abstracts* **30**, 173–175.
- Report of the Round Robin Test carried out by RILEM TC 148-SSC (1997). Strain softening of concrete in uniaxial compression. *Materials and Structures* **30**, 195–209.
- Turcotte, D.L. (1992). *Fractals and Chaos in Geology and Geophysics*, Cambridge University Press.
- van Mier, J.G.M. (1986). Multi axial strain-softening of concrete: part i: fracture and part ii: load histories. *Materials and Structures* **19**, 179–200.
- van Mier, J.G.M. (1996). *Fracture Process of Concrete*, CRC Press, Boca Raton, FL.
- van Vliet, M. and van Mier, J.G.M. (1996). Experimental investigation of concrete fracture under uniaxial compression. *Mechanics of cohesive-frictional materials* **1**, 115–127.